

# Suppression of NYVAC Infection in HeLa Cells Requires RNase L but Is Independent of Protein Kinase R Activity

Mercedes Fernández-Escobar,<sup>a</sup> José Luis Nájera,<sup>b</sup> Sara Baldanta,<sup>a</sup> Dolores Rodriguez,<sup>b</sup> Michael Way,<sup>c</sup> Mariano Esteban,<sup>b</sup> Susana Guerra<sup>a</sup>

Department of Preventive Medicine, Public Health and Microbiology, Universidad Autónoma, Madrid, Spain<sup>a</sup>; Department of Molecular and Cell Biology, Centro Nacional de Biotecnología, Consejo Superior de Investigaciones Científicas, Campus Universidad Autónoma, Madrid, Spain<sup>b</sup>; Cellular Signalling and Cytoskeletal Function, Francis Crick Institute, London, United Kingdom<sup>c</sup>

**Protein kinase R (PKR) and RNase L are host cell components that function to contain viral spread after infections. In this study, we analyzed the role of both proteins in the abortive infection of human HeLa cells with the poxvirus strain NYVAC, for which an inhibition of viral *A27L* and *B5R* gene expression is described. Specifically, the translation of these viral genes is independent of PKR activation, but their expression is dependent on the RNase L activity.**

NYVAC is a vaccinia virus (VACV) strain that is replication incompetent in most human cells and is currently being used as a recombinant poxvirus vaccine vector against multiple diseases (for a review, see reference 1). One of the advantages of replication-deficient viruses is their safety profile, which makes them excellent vehicles for vaccination purposes. However, it has been postulated that the efficacy of replication-incompetent viruses, like NYVAC, is limited by their failure to replicate and the consequent limitation in antigen accumulation during virus infection (1). It has been described that during the course of NYVAC infection in human HeLa cells, there is a late translational blockage that correlates with a marked increase in apoptosis (2, 3). An increase in the phosphorylation status of the translation initiation factor eIF2 $\alpha$  (the  $\alpha$  subunit of eukaryotic initiation factor 2) is associated with this inhibition of protein synthesis during NYVAC infection. In particular, late viral proteins such as those encoded by *A27L* (A27 protein), *A17L* (A17 protein), *B5R* (B5 protein), and *L1R* (L1 protein) genes are not detected in HeLa cells infected with NYVAC, while other non-late viral proteins, such as those encoded by *E3L* (E3 protein) or *A4L* (A4 protein) or the early and late *A36R* (A36 protein) open reading frames (ORFs) are synthesized (2, 3). To understand what leads to the lack of these proteins, we have analyzed which step in the viral life cycle is blocked in NYVAC-infected HeLa cells. We compared viral protein synthesis in HeLa cells infected with either NYVAC or the replication-competent WR VACV strain, using Western blot analysis with specific antibodies for some early (E3 and A36) and late (B5 and A27) viral proteins. As shown in Fig. 1A, the early proteins E3 and A36 were detected in both WR- and NYVAC-infected cells, and their expression was maintained throughout the infection. In contrast, the late proteins B5 and A27 were only detected in WR-infected HeLa cells, indicating a block in their expression during NYVAC infection. The levels of early viral proteins were quite similar with both viruses at 2 h postinfection (hpi), but with longer times postinfection, the levels of E3 and A36 were diminished in NYVAC-infected cells due to the severe blockage in protein translation due to phosphorylation of the initiation factor eIF2 $\alpha$ , as previously published (2, 3). These results were confirmed by immunofluorescence analysis (data not shown) and are consistent with previous results obtained in human dendritic cells (DCs) and macro-

phages infected with NYVAC, in which the late proteins A17 and A27 were not detected in infected cell lysates (4, 5).

Some VACV viral proteins, such as B5, are involved in virion formation, in particular in the intracellular enveloped virus (IEV) assembly and subsequent actin tail formation, which helps to enhance virus dissemination and pathogenesis (6–10). The mechanism of VACV actin tail formation has been intensively investigated with different VACV viruses (11), but not with NYVAC. Although the A33 and A36 transmembrane proteins are both required for actin tail formation, only A36 has been shown to have a direct role in this process (9–12). *A36R* is highly conserved in *Orthopoxvirus* genomes, suggesting that virus-induced actin polymerization at the plasma membrane is widely used by mammalian poxviruses to enhance their cell-to-cell spread (11). Deletion of the *A36R* gene and loss of A36 expression does not affect IEV assembly, but they do lead to an absence of actin tail formation and a small plaque size phenotype, indicative of a defect in viral spread (9, 10, 13). The phosphorylation of Tyr112 and Tyr132 in A36 by Src and Abl family kinases results in the recruitment of the adaptor proteins Nck, WIP, N-WASP, and Grb2, which in turn leads to activation of the Arp2/3 complex and the nucleation of actin polymerization (11, 12, 14). Mutations of Tyr112 and Tyr132 result in a loss of actin tail formation and in a reduction in plaque size (15). It has also been shown that the A36 protein interacts with A33 and that this interaction is required for the incorporation of the former into IEV membranes (16).

To study the effect of the absence of B5 viral late protein expression after NYVAC infection, we examined actin tail forma-

Received 9 October 2015 Accepted 25 November 2015

Accepted manuscript posted online 9 December 2015

Citation Fernández-Escobar M, Nájera JL, Baldanta S, Rodríguez D, Way M, Esteban M, Guerra S. 2016. Suppression of NYVAC infection in HeLa cells requires RNase L but is independent of protein kinase R activity. *J Virol* 90:2135–2141. doi:10.1128/JVI.02576-15.

Editor: R. M. Sandri-Goldin

Address correspondence to Susana Guerra, susana.guerra@uam.es.

M.F.-E., J.L.N., and S.B. contributed equally to this work.

Copyright © 2016, American Society for Microbiology. All Rights Reserved.

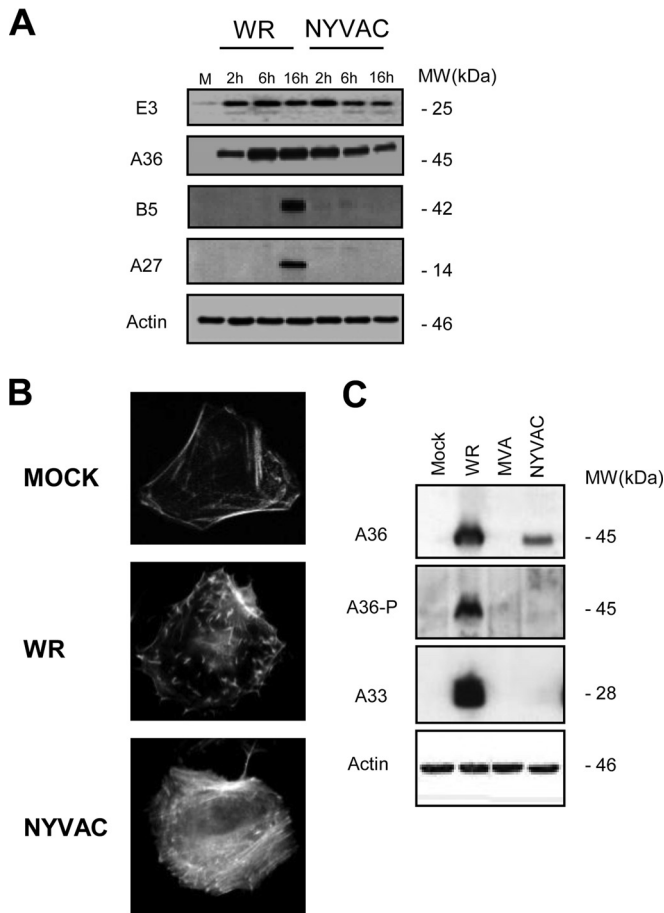


**FIG 1** NYVAC produces an abortive infection in HeLa cells. (A) Viral protein expression in NYVAC-infected HeLa cells. HeLa cells were mock infected (M) or infected with WR or NYVAC (5 PFU/cell). At the indicated times postinfection, cells were harvested and equal amounts of proteins from cell extracts were fractionated by SDS-PAGE, transferred to nitrocellulose, and treated with specific antibodies to early (E3 and A36) and late (B5 and A27) viral proteins. Actin was used as a loading control. The molecular masses (“MW”; in kilodaltons) are indicated and were determined based on protein standards. (B) Blockage in actin tail formation after infection with NYVAC. Mock-infected and WR- or NYVAC-infected HeLa cells (5 PFU/cell) were fixed and stained using phalloidin coupled to tetramethylrhodamine B isothiocyanate at 24 hpi for actin tail detection. Cells were visualized by confocal immunofluorescence microscopy. The images show representative fields. Magnification,  $\times 73$ . (C) Cellular extracts from HeLa cells that were mock infected or infected with NYVAC, MVA, or WR viruses (5 PFU/cell) were collected at 10 hpi into a buffer containing 1 mM sodium orthovanadate. The extracts were analyzed by Western blotting using the 4G10 monoclonal P-Tyr antibody to detect phosphorylated A36 levels produced after the infection, and results were compared to those of the total A36. Additionally, A33 expression was determined by Western blotting. The truncated form of A33R after MVA infection is not shown in the gel. Actin was used as a loading control.

tion, as the presence of B5 is a requirement for IEV production. HeLa cells were infected with WR or NYVAC (5 PFU/cell), and the actin cytoskeleton was visualized by phalloidin staining at 24 hpi. WR-infected cells had characteristic actin tails (Fig. 1B). In contrast, no actin tails were detected in NYVAC-infected cells. As the tyrosine phosphorylation (P-Tyr) of A36 mediated by Src and Abl family kinases is essential for the nucleation of actin polymerization, we analyzed the A36 phosphorylation levels after infection with WR and NYVAC. We also examined the presence of A33,

since both proteins are necessary for the production of actin tails. Cellular extracts of HeLa cells infected with NYVAC, MVA, or WR strains (5 PFU/cell) at 10 hpi were collected using a buffer containing 1 mM sodium orthovanadate and were analyzed by Western blotting using the 4G10 anti-P-Tyr monoclonal antibody to detect tyrosine-phosphorylated A36. Additionally, A33 expression was also determined by Western blotting. As shown in Fig. 1C, phosphorylation of A36 was not observed in NYVAC-infected cells, and it is noteworthy that the early A33 protein was also not detected. Together, these results demonstrate that during NYVAC infection in HeLa cells, several viral proteins (A33 [Fig. 1C] and A27 and B5 [Fig. 1A]) are not produced. While A36 is produced, it is not phosphorylated. To study if the absence of B5 after NYVAC infection is due to a mutation in its viral gene or to the restriction by a cellular host range gene, we analyzed the levels of B5 protein following coinfection of HeLa cells with NYVAC and the WR VV $\Delta$ B5R deletion mutant of VACV, which lacks the B5R gene. HeLa cells were infected with a total of 5 PFU/cell of NYVAC and VV $\Delta$ B5R, and at the indicated times postinfection, B5 protein expression was analyzed by Western blotting. As shown in Fig. 2A, B5 was detected at 16 h postcoinfection, indicating that the B5R gene from the NYVAC genome can be transcribed and translated correctly in the presence of the replication-competent VV $\Delta$ B5R strain. Next, we sought to determine if under these conditions actin tail formation was restored. Cells were infected with NYVAC or VV $\Delta$ B5R or coinfecting with both viruses (2.5 PFU/cell of each virus), and the actin cytoskeleton was visualized by phalloidin staining at 24 hpi. The coinfecting cells had characteristic actin tails (Fig. 2B), indicating the rescue of IEV formation. In contrast, no actin tails were detected in NYVAC-infected cells or in VV $\Delta$ B5R-infected cells. Moreover, the presence of B5 and A36 proteins in the coinfecting cells was detected with specific antibodies. These findings suggested that the blockade of viral proteins in NYVAC-infected HeLa cells must be associated with a specific translational inhibitor that remains active during NYVAC infection but whose activity is blocked in WR-infected cells.

During viral infections, double-stranded RNA (dsRNA) is produced, which triggers the subsequent induction of type I interferon (IFN). This enhances transcription of genes encoding protein kinase R (PKR) and the 2',5'-oligoadenylate synthetase (2-5A synthetase)/RNase L enzymes, among others (17). Double-stranded RNA (dsRNA) then binds to and activates PKR and the 2-5A-synthetase, leading to suppression of translation initiation and to RNA degradation by RNase L, respectively. PKR is also involved in the regulation of signal transduction, apoptosis, cell proliferation, and differentiation (17). PKR inhibits viral replication via phosphorylation of eIF2 $\alpha$ , which impairs the recycling of eIF2S1 between successive rounds of translation initiation, leading to inhibition of this process and eventually to shutdown of cellular and viral protein synthesis (17, 18). In addition, 2-5A synthetase produces short, 2',5'-linked oligoadenylates, which activate RNase L, a single-stranded specific endoribonuclease that degrades mRNA and rRNA, thus controlling major pathogenic processes (19). We were interested in determining the effects of PKR and RNase L on NYVAC infection, and in particular, in investigating whether these proteins were responsible for the abortive replication of NYVAC in HeLa cells.

As we discussed above, in NYVAC-infected HeLa cells the specific blockage in the translation of viral proteins is accompanied by eIF2 $\alpha$  phosphorylation and apoptosis (2, 3), suggesting that PKR

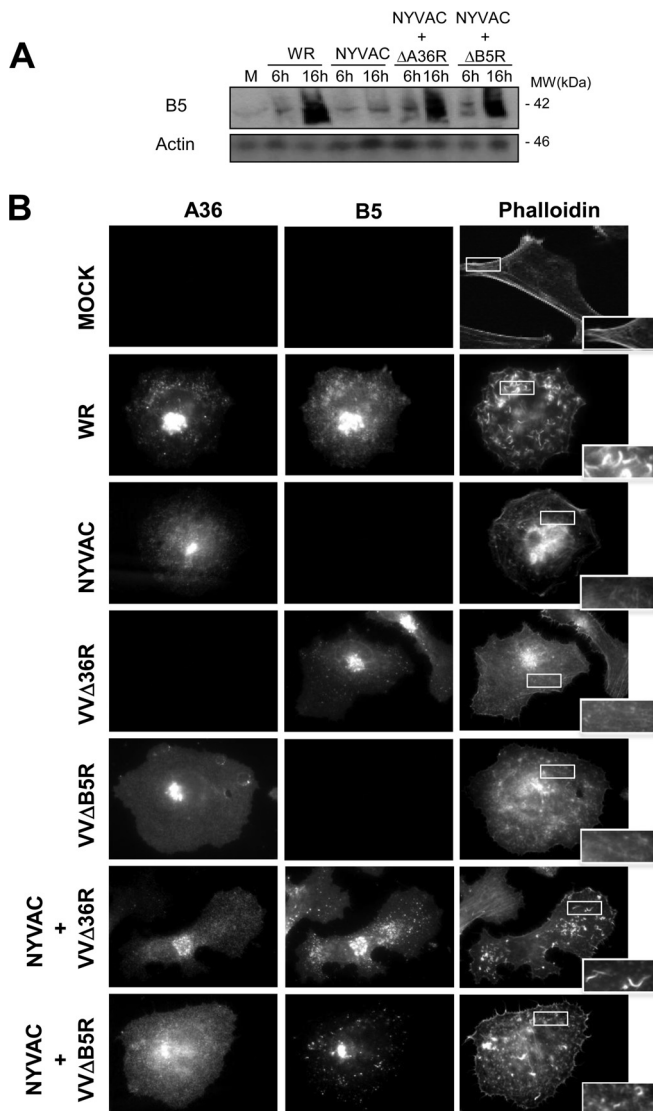


**FIG 2** B5R expression and actin tail formation are restored after NYVAC and VV $\Delta B5R$  coinfection. (A) HeLa cells were mock infected (M) or infected with WR or NYVAC (5 PFU/cell), or coinfecting with NYVAC and VV $\Delta A36R$  (2.5 PFU/cell per each virus) or NYVAC and VV $\Delta B5R$  (2.5 PFU/cell per each virus). At the indicated times postinfection, equal amounts of proteins from cell extracts were fractionated by SDS-PAGE, transferred onto nitrocellulose, and treated with specific antibodies to the B5 late viral protein. Actin was used as a loading control. Molecular masses ("MW"; in kilodaltons) are indicated and were determined based on protein standards. (B) Restoration of actin tail formation after the coinfection with NYVAC and VV $\Delta B5R$ . HeLa cells were mock infected (M) or infected with WR, NYVAC, VV $\Delta A36R$ , or VV $\Delta B5R$  (5 PFU/cell), or coinfecting with NYVAC and VV $\Delta A36R$  (2.5 PFU/cell per each virus) or NYVAC and VV $\Delta B5R$  (2.5 PFU/cell per each virus). Actin tails were stained using phalloidin-tetramethylrhodamine B isothiocyanate at 24 hpi and visualized by confocal microscopy. Viral proteins B5 and A36 were visualized using specific antibodies. The images show representative fields. Magnification,  $\times 73$ .

could be activated. Taking into account that in response to many viral infections PKR becomes activated (17), we wanted to test the role of PKR in the NYVAC replication defect in HeLa cells. HeLa cells deficient in PKR (HeLa-siPKR) generated by an RNA interference-silencing strategy and control cells (HeLa-siCTR) were

infected with NYVAC. We then examined viral protein expression, and although we detected early proteins (E3 and A36) in both cell types, late proteins were not observed (A27 and B5) in either PKR-expressing or PKR-deficient cells. Phosphorylation of eIF2 $\alpha$  was, however, observed even in the absence of PKR (Fig. 3A), indicating that PKR is not the activated kinase involved in this process after NYVAC infection. These results demonstrate that the inhibition of the translation of viral proteins and viral replication in NYVAC-infected HeLa cells is independent of PKR activity (Fig. 3A and B). Since the activation of PKR has previously been shown to lead to induction of apoptosis with other VACV strains (20), and NYVAC induces apoptosis following infection of HeLa cells, we next assayed the ability of NYVAC to induce apoptosis in PKR-deficient HeLa cells. Inspection of HeLa-siCTR and HeLa-siPKR cells infected with NYVAC by phase-contrast microscopy showed that both cell lines exhibited morphological changes characteristic of cells undergoing apoptosis (Fig. 3C). To confirm our microscope observations, we used an antibody that recognizes both full-length and cleaved poly(ADP-ribose) polymerase 1 (PARP-1) to assess apoptosis in HeLa-siCTR or HeLa-siPKR cells infected with NYVAC. In both cases, the cleaved PARP-1 fragment of 89 kDa was evident at 16 hpi (Fig. 3D), indicating that NYVAC is capable of inducing apoptosis in the absence of PKR. Similar results were obtained when we measured the level of apoptosis activation with a caspase-Glo 3/7 assay kit (Fig. 3E). These results demonstrated that apoptosis triggered by NYVAC infection in HeLa cells is not due to PKR activation and, thus, additional apoptotic routes must be regulated following infection. Together, these results indicate that the NYVAC phenotype is different from that observed for the VV $\Delta E3L$  mutant virus that lacks the viral protein E3, which induces eIF2 $\alpha$  phosphorylation and apoptosis (17) in a PKR-dependent manner (20). Furthermore, PKR also plays a major role in restricting the attenuated MVA poxvirus strain (21). This is probably due to the differences between the genomes of these viruses in encoding inhibitors of the IFN regulatory pathways (22).

As mentioned before, RNase L is another important enzyme regulated by IFN that exerts its activity at multiple levels, including the degradation of viral and host RNA, as well as induction of apoptosis (23, 24). Furthermore, host and viral RNAs cleaved by RNase L function as ligands for RIG-I and MDA5 in amplifying type I interferon expression and antiviral responses (23, 25). Several viruses have mechanisms to directly counteract RNase L activity (24). We previously showed that in HeLa cells, NYVAC infection triggers rRNA degradation late in infection, with the same cleavage pattern observed during activation of the RNase L system (3). To obtain evidence that RNase L has an effect in NYVAC replication, we used HeLa cells expressing wild-type RNase L (HeLa and HeLa-M-W12) or HeLa cells expressing a dominant negative mutant RNase L (named HeLa-M-M25; kindly provided by R. H. Silverman).

We first examined rRNA integrity in NYVAC-infected HeLa, HeLa-M-W12, or HeLa-M-M25 cells. Total RNA was isolated from infected and mock-infected cells and fractionated by formaldehyde-agarose gel electrophoresis. As expected, rRNA degradation was observed in those cells that express parental RNase L (HeLa and HeLa-M-W12). In contrast, in HeLa-M-M25 cells, that express a dominant negative mutant RNase L, no breakdown of 28S and 18S rRNAs was observed after NYVAC infection (Fig. 4A). This result indicated that the rRNA degradation after NYVAC infection is



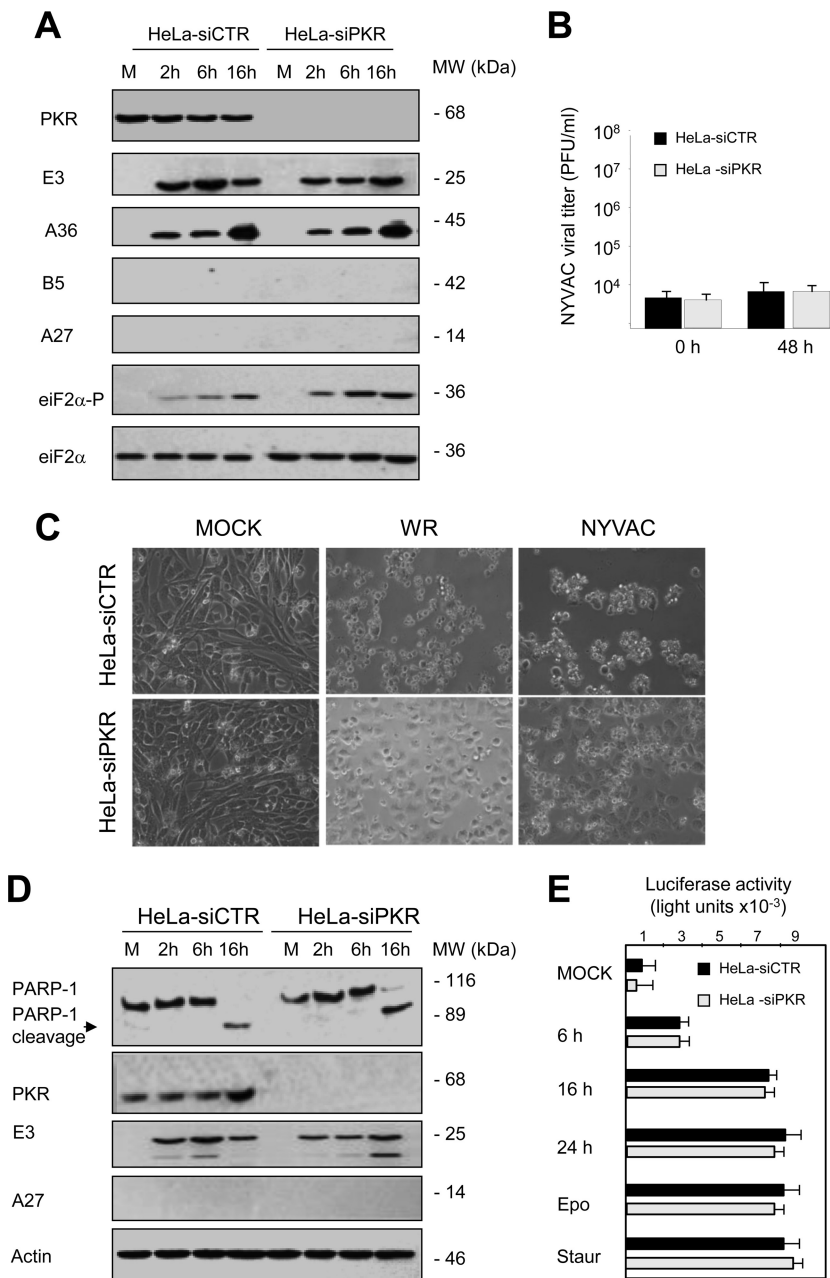


**FIG 3** Protein synthesis, apoptosis induction, and eIF2 $\alpha$  phosphorylation in HeLa-siCTR and HeLa-siPKR cells infected with NYVAC. (A) Viral protein expression during NYVAC infection. HeLa-siCTR or HeLa-siPKR cells were mock infected (M) or infected with NYVAC (5 PFU/cell). At the indicated times postinfection, equal amounts of proteins from cell extracts were fractionated by SDS-PAGE, transferred to nitrocellulose, and treated with specific antibodies to virus early proteins (E3 and A36) and late proteins (B5 and A27). The levels of PKR, eIF2 $\alpha$ , and phosphorylated eIF2 $\alpha$  were visualized by using specific antibodies, and actin was used as a loading control. Molecular masses (“MW”; in kilodaltons) are indicated and were determined based on protein standards. (B) Cells were infected (0.01 PFU/cell) and at the different times indicated, cells were harvested and virus yields were determined by plaque assay. Results represent the means  $\pm$  the standard deviations of three independent experiments. *P* values from a two-tailed *t* test, assuming nonequal variance, were determined. In all cases, we obtained *P* values of  $<0.01$ . (C) Apoptosis induction during NYVAC infection in HeLa cells is a PKR-independent process. HeLa-siCTR or HeLa-siPKR cells were mock infected (M) or infected with WR or NYVAC (5 PFU/cell). At the indicated times postinfection, apoptosis was assessed via phase-contrast microscopy. NYVAC-infected cells showed characteristic apoptosis, defined by a rounded, floating, phase-bright, wrinkled shape. (D) Time course of PARP-1 cleavage during NYVAC infection. HeLa-siCTR or HeLa-siPKR cells were mock infected (M) or infected with NYVAC (5 PFU/cell). At the indicated times postinfection, cells were harvested and equal amounts of proteins from cell extracts were fractionated by SDS-PAGE, transferred to nitrocellulose, and immunoblotted with antibodies against PARP-1 and against virus early (E3) and late (A27) proteins. An 89-kDa PARP-1 cleavage product was observed at 16 hpi in both cell lines. Molecular masses (“MW”; in kilodaltons) are indicated and are based on protein standards. PKR levels were visualized using a specific anti-PKR antibody, and actin was used as a loading control. (E) Quantification of apoptotic cells after NYVAC infection. HeLa-siCTR or HeLa-siPKR cells were mock infected (M) or infected with NYVAC (5 PFU/cell), and at 6, 16, and 24 hpi, cells were fixed and processed to quantify apoptosis by using a caspase-Glo 3/7 assay kit. Etoposide and staurosporine treatments were used as apoptosis activators. Results represent the means  $\pm$  the standard deviations from three independent experiments. *P* values from a two-tailed *t* test assuming nonequal variance were determined. In all cases, we obtained *P* values of  $<0.05$ .

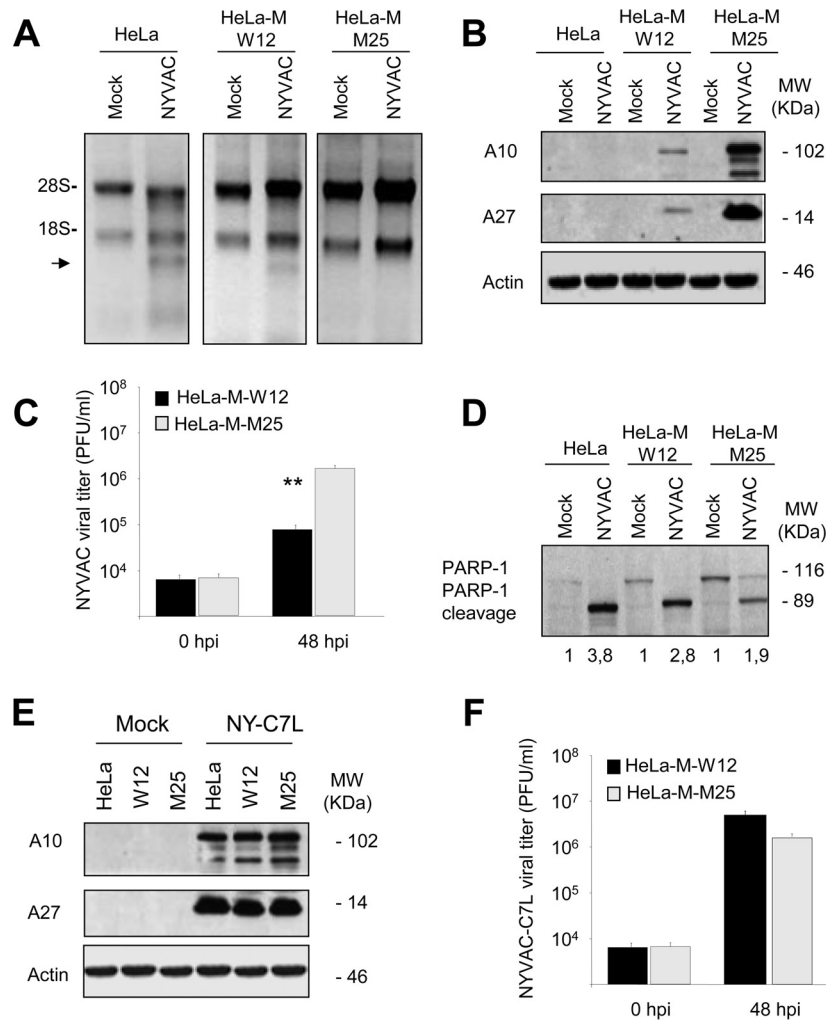


**FIG 4** RNA degradation, protein synthesis, virus growth, and apoptosis induction in HeLa, HeLa-M-W12, or HeLa-M-M25 cells infected with NYVAC. (A) HeLa, HeLa-M-W12, and HeLa-M-M25 cells were mock infected (M) or infected with NYVAC (5 PFU/cell). Total rRNA was isolated from cells uninfected or infected with NYVAC at 16 hpi; 2  $\mu$ g of each sample was applied for electrophoresis, and the gel was stained with ethidium bromide. (B) Viral protein expression during NYVAC infection. HeLa, HeLa-M-W12, and HeLa-M-M25 cells were mock infected (M) or infected with NYVAC (5 PFU/cell). Cells were harvested at 16 hpi, and equal amounts of proteins from cell extracts were fractionated by SDS-PAGE, transferred to nitrocellulose, and treated with specific antibodies to A10 or A27 viral proteins. Actin was used as a loading control. Molecular masses (“MW”; in kilodaltons) are indicated and are based on protein standards. (C) Cells were infected, and at the different times indicated cells were harvested and virus yields were determined by plaque assay. Results represent the means  $\pm$  the standard deviations of three independent experiments. *P* values from a two-tailed *t* test assuming nonequal variance were determined. In all cases, we obtained *P* values of  $<0.01$ . (D) PARP-1 cleavage during NYVAC infection. HeLa, HeLa-M-W12, and HeLa-M-M25 cells were mock infected (M) or infected with NYVAC (5 PFU/cell). At 16 hpi, cells were harvested and equal amounts of proteins from cell extracts were fractionated by SDS-PAGE, transferred to nitrocellulose, and immunoblotted with anti-PARP-1 antibodies. Numbers appearing under each lane represent the ratio of the intensity of the band corresponding to the PARP-1 cleaved fragments in infected cells to those levels in uninfected cells, as determined by densitometric analysis. Molecular masses (“MW”; in kilodaltons) are indicated and are based on protein standards. (E) HeLa, HeLa-M-W12, and HeLa-M-M25 cells were mock infected (M) or infected with NYVAC-C7L (5 PFU/cell). At 16 hpi, cells were collected and equal amounts of proteins from cell extracts were fractionated by SDS-PAGE, transferred to nitrocellulose, and treated with specific antibodies to A10 or A27 viral proteins. Actin was used as a loading control. (F) HeLa-M-W12 and HeLa-M-M25 cells were infected with NYVAC-C7L, and at the different times indicated cells were harvested and virus yields were determined by plaque assay. Results represent the means  $\pm$  the standard deviations of three independent experiments. *P* values from a two-tailed *t* test assuming nonequal variance were determined. In all cases, we obtained *P* values of  $<0.01$ .

RNase L dependent. When we examined late (A10 and A27) viral protein expression in NYVAC-infected HeLa, HeLa-M-W12, or HeLa-M-M25 cells, we observed total or a nearly complete absence of these late proteins in cells that express wild-type RNase L. In contrast, we observed high levels of late viral protein production in HeLa-M-M25 cells, indicating that RNase L is involved in the translational control of late proteins in NYVAC infection (Fig. 4B). Moreover, the presence of late viral proteins correlated with

the capacity of NYVAC to grow in HeLa-M-M25 cells (Fig. 4C). Finally, we evaluated apoptosis activation in HeLa, HeLa-M-W12, and HeLa-M-M25 cells infected with NYVAC. PARP-1 cleavage was considerably decreased after the infection of the HeLa-M-M25 cells (Fig. 4D). When the apoptosis was quantified by densitometric analysis of the cleaved protein bands, a significant reduction was observed after infection of the cells that do not express RNase L, compared with infected HeLa or HeLa-M-W12 cells.

While the band corresponding to the cleaved PARP-1 fragment in infected HeLa-M-M25 cells was 1.9 times more intense than the same band in mock-infected cells, in infected HeLa and HeLa-M-W12 cells, this band was 3.8 and 2.8 times more intense with respect to the corresponding mock-infected cells. This result indicates that the apoptosis induced by NYVAC in HeLa cells is RNase L dependent. It has been previously demonstrated that the presence of the viral gene C7L restores the NYVAC capacity to replicate in HeLa cells at a similar rate as the WR strain (3). Then, we infected HeLa, HeLa-M-W12, and HeLa-M-M25 cells with a NYVAC recombinant expressing C7L (named NYVAC-C7L) and showed that late viral protein production and virus growth were rescued in HeLa cells expressing wild-type RNase L (Fig. 4E and F). Lastly, we also measured the viral growth with NYVAC and NYVAC-C7L in murine embryonic fibroblast (MEFs) from RNase L<sup>+/+</sup> and RNase L<sup>-/-</sup> mice, and the results in these murine cells were comparable to those obtained in HeLa cells (data not shown). As shown here, the replication capacity of NYVAC-C7L for overcoming the RNase L activity suggests a direct or indirect role of C7L in blocking RNase L.

In summary, while the poxvirus vaccine candidate NYVAC has a host-restricted replication phenotype in most human cells, the mechanism of restriction has remained elusive. In this study, we showed that after infection of HeLa cells with NYVAC there is a blockage in the translation of some viral proteins, and that this is accompanied by an inhibition in the production of actin tails. Through complementation assays with specific defective viruses, we showed that the genes encoding late viral proteins are still capable of being transcribed and translated “in *trans*” from the genome of NYVAC, indicating that the viral restriction is related to cellular factors. We studied two cellular factors with an essential function in the replication of viruses and pathological processes, PKR and RNase L. We showed that PKR does not exert a regulatory role in NYVAC growth, but RNase L is an essential host restriction factor for NYVAC. Since the *E3L* and *K3L* genes (26) involved in RNase L inhibition remain intact in the NYVAC genome, these results suggest that there are additional viral genes, such as C7L, that control the action of RNase L.

## ACKNOWLEDGMENTS

We thank Mark Dodding for his help with the phosphorylation assay and for critical reviews of the manuscript. We thank R. H. Silverman for the RNase L mutant HeLa cells and B. L. Jacobs for the generous gift of the rabbit E3 antibody. We also thank Beatriz Martín and Victoria Jimenez for excellent technical assistance.

This work was supported by grants from the Spanish Ministry of Health (FIS2011-00127) and Bayer Group Grants4Grants (2013-08-0982 to S.G., SAF2008-02036 to M.E., and AGL2010-15495 to D.R.).

## FUNDING INFORMATION

Spanish Ministry of Health provided funding to Susana Guerra under grant number FIS2011-00127 t.

## REFERENCES

- Gomez CE, Najera JL, Krupa M, Perdiguero B, Esteban M. 2011. MVA and NYVAC as vaccines against emergent infectious diseases and cancer. *Curr Gene Ther* 11:189–217. <http://dx.doi.org/10.2174/156652311795684731>.
- Guerra S, Lopez-Fernandez LA, Pascual-Montano A, Najera JL, Zaballos A, Esteban M. 2006. Host response to the attenuated poxvirus vector NYVAC: upregulation of apoptotic genes and NF- $\kappa$ B-responsive genes in infected HeLa cells. *J Virol* 80:985–998. <http://dx.doi.org/10.1128/JVI.80.2.985-998.2006>.
- Najera JL, Gomez CE, Domingo-Gil E, Gherardi MM, Esteban M. 2006. Cellular and biochemical differences between two attenuated poxvirus vaccine candidates (MVA and NYVAC) and role of the C7L gene. *J Virol* 80:6033–6047. <http://dx.doi.org/10.1128/JVI.02108-05>.
- Guerra S, Najera JL, Gonzalez JM, Lopez-Fernandez LA, Climent N, Gatell JM, Gallart T, Esteban M. 2007. Distinct gene expression profiling after infection of immature human monocyte-derived dendritic cells by the attenuated poxvirus vectors MVA and NYVAC. *J Virol* 81:8707–8721. <http://dx.doi.org/10.1128/JVI.00444-07>.
- Royo S, Sainz B, Jr, Hernandez-Jimenez E, Reyburn H, Lopez-Collazo E, Guerra S. 2014. Differential induction of apoptosis, interferon signaling, and phagocytosis in macrophages infected with a panel of attenuated and nonattenuated poxviruses. *J Virol* 88:5511–5523. <http://dx.doi.org/10.1128/JVI.00468-14>.
- Herrera E, Lorenzo MM, Blasco R, Isaacs SN. 1998. Functional analysis of vaccinia virus B5R protein: essential role in virus envelopment is independent of a large portion of the extracellular domain. *J Virol* 72:294–302.
- Katz E, Wolffe E, Moss B. 2002. Identification of second-site mutations that enhance release and spread of vaccinia virus. *J Virol* 76:11637–11644. <http://dx.doi.org/10.1128/JVI.76.22.11637-11644.2002>.
- Mathew E, Sanderson CM, Hollinshead M, Smith GL. 1998. The extracellular domain of vaccinia virus protein B5R affects plaque phenotype, extracellular enveloped virus release, and intracellular actin tail formation. *J Virol* 72:2429–2438.
- Rottger S, Frischknecht F, Reckmann I, Smith GL, Way M. 1999. Interactions between vaccinia virus IEV membrane proteins and their roles in IEV assembly and actin tail formation. *J Virol* 73:2863–2875.
- Sanderson CM, Frischknecht F, Way M, Hollinshead M, Smith GL. 1998. Roles of vaccinia virus EEV-specific proteins in intracellular actin tail formation and low pH-induced cell-cell fusion. *J Gen Virol* 79:1415–1425. <http://dx.doi.org/10.1099/0022-1317-79-6-1415>.
- Leite F, Way M. 2015. The role of signalling and the cytoskeleton during vaccinia virus egress. *Virus Res* 209:87–99. <http://dx.doi.org/10.1016/j.virusres.2015.01.024>.
- Frischknecht F, Moreau V, Rottger S, Gonfloni S, Reckmann I, Superti-Furga G, Way M. 1999. Actin-based motility of vaccinia virus mimics receptor tyrosine kinase signalling. *Nature* 401:926–929. <http://dx.doi.org/10.1038/44860>.
- Wolffe EJ, Weisberg AS, Moss B. 1998. Role for the vaccinia virus A36R outer envelope protein in the formation of virus-tipped actin-containing microvilli and cell-to-cell virus spread. *Virology* 244:20–26. <http://dx.doi.org/10.1006/viro.1998.9103>.
- Welch MD, Way M. 2013. Arp2/3-mediated actin-based motility: a tail of pathogen abuse. *Cell Host Microbe* 14:242–255. <http://dx.doi.org/10.1016/j.chom.2013.08.011>.
- Ward BM, Moss B. 2001. Vaccinia virus intracellular movement is associated with microtubules and independent of actin tails. *J Virol* 75:11651–11663. <http://dx.doi.org/10.1128/JVI.75.23.11651-11663.2001>.
- Wolffe EJ, Weisberg AS, Moss B. 2001. The vaccinia virus A33R protein provides a chaperone function for viral membrane localization and tyrosine phosphorylation of the A36R protein. *J Virol* 75:303–310. <http://dx.doi.org/10.1128/JVI.75.1.303-310.2001>.
- Garcia MA, Gil J, Ventoso I, Guerra S, Domingo E, Rivas C, Esteban M. 2006. Impact of protein kinase PKR in cell biology: from antiviral to anti-proliferative action. *Microbiol Mol Biol Rev* 70:1032–1060. <http://dx.doi.org/10.1128/MMBR.00027-06>.
- Donnelly N, Gorman AM, Gupta S, Samali A. 2013. The eIF2 $\alpha$  kinases: their structures and functions. *Cell Mol Life Sci* 70:3493–3511. <http://dx.doi.org/10.1007/s00018-012-1252-6>.
- Malathi K, Paranjape JM, Bulanova E, Shim M, Guenther-Johnson JM, Faber PW, Eling TE, Williams BR, Silverman RH. 2005. A transcriptional signaling pathway in the IFN system mediated by 2'-5'-oligoadenylate activation of RNase L. *Proc Natl Acad Sci U S A* 102:14533–14538. <http://dx.doi.org/10.1073/pnas.0507551102>.
- Zhang P, Jacobs BL, Samuel CE. 2008. Loss of protein kinase PKR expression in human HeLa cells complements the vaccinia virus E3L deletion mutant phenotype by restoration of viral protein synthesis. *J Virol* 82:840–848. <http://dx.doi.org/10.1128/JVI.01891-07>.
- Backes S, Sperling KM, Zwilling J, Gasteiger G, Ludwig H, Kremmer E, Schwantes A, Staib C, Sutter G. 2010. Viral host-range factor C7 or K1 is essential for modified vaccinia virus Ankara late gene expression in human

- and murine cells, irrespective of their capacity to inhibit protein kinase R-mediated phosphorylation of eukaryotic translation initiation factor 2 $\alpha$ . *J Gen Virol* 91:470–482. <http://dx.doi.org/10.1099/vir.0.015347-0>.
22. **Perdiguero B, Esteban M.** 2009. The interferon system and vaccinia virus evasion mechanisms. *J Interferon Cytokine Res* 29:581–598. <http://dx.doi.org/10.1089/jir.2009.0073>.
  23. **Malathi K, Saito T, Crochet N, Barton DJ, Gale M, Jr, Silverman RH.** 2010. RNase L releases a small RNA from HCV RNA that refolds into a potent PAMP. *RNA* 16:2108–2119. <http://dx.doi.org/10.1261/rna.2244210>.
  24. **Silverman RH.** 1994. Fascination with 2-5A-dependent RNase: a unique enzyme that functions in interferon action. *J Interferon Res* 14:101–104. <http://dx.doi.org/10.1089/jir.1994.14.101>.
  25. **Malathi K, Dong B, Gale M, Jr, Silverman RH.** 2007. Small self-RNA generated by RNase L amplifies antiviral innate immunity. *Nature* 448:816–819. <http://dx.doi.org/10.1038/nature06042>.
  26. **Rice AD, Turner PC, Embury JE, Moldawer LL, Baker HV, Moyer RW.** 2011. Roles of vaccinia virus genes E3L and K3L and host genes PKR and RNase L during intratracheal infection of C57BL/6 mice. *J Virol* 85:550–567. <http://dx.doi.org/10.1128/JVI.00254-10>.